

RERTR 2014 – 35th INTERNATIONAL MEETING ON
REDUCED ENRICHMENT FOR RESEARCH AND TEST REACTORS

OCTOBER 12-16, 2014
IAEA VIENNA INTERNATIONAL CENTER
VIENNA, AUSTRIA

**Intelligent Integrated Machining: Zr Thickness Measurements using
XRF for Process Control and Quality Assurance**

D. A. Summa¹, V. M. Lopez², G. J. Havrilla², D. E. Dombrowski³

¹Applied Engineering Technology Division

²Chemistry Division

³Materials Science and Technology Division

Los Alamos National Laboratory, PO Box 1663, Los Alamos, NM 87544 - USA

ABSTRACT

Reactor operation is dependent upon precise control of fuel plate geometry and thickness of individual layers, however there is currently no method to assess Zr diffusion barrier thickness over the entire surface area of the foil. An energy-dispersive x-ray fluorescence spectrometry (XRF) technique was developed to map Zr coating thickness over the surfaces of co-rolled fuel foils. Two different instruments and calibration methods were employed. An inexpensive handheld XRF analyzer was chosen for rapid non-destructive estimation of Zr coating and/or Al cladding thickness *in situ* on the shop floor, while a laboratory-grade scanning macro-XRF was used to confirm the handheld measurements and for R&D applications. For Zr foil calibration standards, results from the handheld analyzer and the macro-XRF instrument are in excellent agreement with each other and within $\pm 5\%$ of known values. The method was successfully applied to map Zr on 48" LEU foils and to study effects of cold-rolling.

1. Introduction

To prevent swelling and possible rupture of monolithic LEU fuel plates due to fission gases produced during reactor operation, current designs call for bonding a thin Zr diffusion barrier to both sides of the U-10Mo fuel meat prior to applying the Al-6061 cladding. To provide an adequate margin of safety, a minimum barrier layer thickness of twice the recoil distance of the fission fragments is desired. For LEU monolithic fuel plates currently under development, the target Zr layer thickness is nominally 25 μm (1 mil) [1-3].

The baseline method for applying the Zr barrier layer is a hot "co-rolling" process that bonds the Zr to the U-10Mo followed by a subsequent cold-rolling operation in which the fuel foil is formed to final thickness. A minimum amount of hot work is crucial for U-Zr bond integrity, while a certain amount of cold work is necessary to provide an adequate Zr surface finish for subsequent cladding operations [4]. Alternative methods such as plasma-spraying, which may provide cost benefit and potentially eliminate technical issues associated with co-rolling, are actively under development [1, 2].

To assess the quality of the final Zr barrier layer, edges of sheared fuel foils are examined using optical and scanning electron microscopy. There is currently no method to assess Zr diffusion barrier thickness that is 1) nondestructive, and 2) capable of mapping Zr thickness over the entire surface area of the foil. To address these issues, energy-dispersive x-ray fluorescence spectrometry (XRF) techniques for measuring Zr coating thickness were developed and demonstrated using two different instruments and calibration procedures. An inexpensive handheld XRF analyzer was chosen for rapid non-destructive estimation of Zr coating and/or Al cladding thickness *in situ* on the shop floor, while a laboratory-grade scanning macro-XRF was used to confirm the handheld measurements and for R&D applications. This paper reviews general principles of XRF, discusses calibration procedures for XRF-based measurements of coating thickness, comparison between the handheld and macroXRF methods including advantages and limitations of each, and presents results from a cold-rolling process optimization study and other applications.

2. Background

X-ray fluorescence spectroscopy, or XRF, is based upon the measurement of emission lines resulting when a material is bombarded with X-rays. When a sufficiently energetic photon collides with an atom, it can dislodge an electron from an inner shell of the atom. The aforementioned “gap” in the inner shell creates an unfavorable excited state; to reduce entropy, an electron from a higher orbital shell immediately “falls” into the gap. During this transition process, a photon with energy equal to the difference in binding energies between the two shells in question is released. The spectral pattern of the released, or fluorescing, X-rays is different for and specific to each element. Thus characteristic x-ray fluorescence “lines” can be used to identify elemental components in a material.

Recent advances in x-ray tube miniaturization coupled with development of small, high-count-rate cryogen-free silicon drift detectors have revolutionized XRF analysis. Although XRF spectroscopy dates back to Roentgen’s accidental discovery of X-rays in 1895, the method remained primarily a lab-based specialty tool due to complex and bulky equipment and long experimental dwell times. In the last few years, however, inexpensive high resolution handheld energy dispersive XRF units have become widely available, bringing rapid, reliable XRF analysis to the field. The low-power systems boast high count rates and excellent energy resolution (120 – 200 eV), albeit coarser spatial resolution when compared to standard laboratory XRF systems. Built-in deconvolution/quantitation software based upon the Method of Fundamental Parameters provides accuracy of greater than 1% in elemental composition [5-9].

Although XRF is not usually marketed as a thickness measurement tool, laboratory XRF systems have been used in both absorption and emission modes to assess the thickness of coatings or cladding layers [10-12]. In cases where there is a base or backing layer capable of producing detectable fluorescence emissions and where the coating or cladding is thin enough for fluorescing x-rays from the base layer to reach the surface (i.e., cladding thickness less than the cladding material saturation thickness for the base material element energy lines), the intensity of the base layer signal decreases as the cladding thickness increases, with the intensity and thickness being related through the Beer-Lambert law. Similarly, relative intensity of fluorescing elements within the cladding itself increases with increasing cladding thickness. Provided the coatings are thin enough to permit detection of at least some signal from the base layer and assuming sampling parameters remain fixed, these principles can be used to construct calibration

curves for thickness assessment. Note that because XRF is an inherently stochastic process, with secondary fluorescence, scattering, transition probabilities, fluorescence yield, etc. all affecting the measured intensities, an empirical calibration procedure is necessary to correlate absolute thickness of the coating or cladding with measured XRF signal intensities. Such calibrations are specific to the material combination in question.

3. Experimental Procedure

3.1 Handheld XRF

The instrument used for these measurements was a commercially-available 35kV, 4W optimized silver-anode Olympus-InnovX α -2000 handheld XRF analyzer with a spot size of 5 mm x 7 mm (Figure 1a). The unit is factory-calibrated to NIST-traceable standards; internal start-up standardization procedures ensure that the unit is operating within acceptable limits. Test time was 10-seconds per measurement. For calibration purposes, a minimum of 10 measurements per sample configuration were taken. The analyzer stores each measured spectra along with count rates at each energy peak. Proprietary software based on the Method of Fundamental Parameters accounts for the source profile, internal source-detector geometry, inter-element interactions, etc., before converting the measured intensities to elemental concentrations, which are available to be exported for offline analysis. The software does not directly export raw count-rates as a function of energy.

Because XRF is insensitive to bonding condition, a simple fuel element surrogate with easily interchangeable parts was created by layering high-purity Zr foils of known thickness over a 20-mil (0.5mm) “infinitely thick” machined DU-10Mo plate. Composition of the Zr foils and the DU-10Mo base material were verified using the handheld XRF instrument in normal operating mode. The thickness of the Zr foils was verified by mechanically measuring with a linear variable differential transformer (LVDT) in conjunction with a set of calibrated precision gauge blocks.

To determine Zr foil thickness in the absence of any aluminum cladding, high-purity Zr foils of known thickness were laid over the bare DU-10Mo alloy and a series of ten to twenty five XRF spectra (10-second count time) were taken for each Zr foil or foil combination. Zr foil thicknesses measured 0.0 – 1.72 mils (0.0 – 0.044 mm); stacking the Zr foils in various combinations yielded 23 different foils or foil combinations in 18 unique thicknesses ranging from 0.0 – 2.20 mils (0.0 – 0.056 mm). For each spectrum the built-in software within the XRF analyzer assigns a sequential reading number and computes a normalized chemistry, reporting all elements detected and the weight percentage of each present in the total. The range of reading numbers corresponding to each Zr foil thickness was recorded. After all data was acquired, elemental composition expressed as a percentage of the total was exported for further analysis.

3.2 MacroXRF

The Los Alamos MacroXRF (mXRF) is a customized conventional laboratory XRF instrument equipped with an expanded sample chamber and precision translational stages to facilitate automated high-resolution scanning XRF capabilities. The instrument (Figure 1b) features a 35kV, 100 μ A rhodium x-ray tube coupled with a liquid-nitrogen cooled lithium drifted silicon detector and a commercial MCA; spot size is 1 mm x 1mm. Unlike handheld instruments, which are designed such that the nose of the instrument is placed either in direct contact with or no more than 2 mm away from the sample, the source/detector pair in the mXRF is fixed at 1-inch

above the sample table. Further details and capabilities of the mXRF system are discussed in reference [13].

To calibrate for Zr thickness measurement, thirteen high-purity Zr foil standards ranging in thickness from 0.04 – 3.0 mil (0.001 – 0.076 mm) were obtained from Goodfellow (Corapolis, PA) and other sources. The manufacturer’s stated thickness tolerances for the Goodfellow foils was $\pm 10\%$ for foils > 0.05 mm (2 mils), $\pm 15\%$ for foils 0.01- 0.05 mm (0.4 - 2 mils), and $\pm 25\%$ for foils < 0.01 mm (0.4 mils). Foils were mounted on a flat DU-10Mo plate with double-sided tape and net spectral intensity was recorded for the Zr- $K_{\alpha 1}$ line was recorded for a 20-second dwell time. All samples were measured in the as-received condition, although efforts were made to ensure individual samples were as flat as possible.



Figure 1: (a) Left- Commercial handheld XRF analyzer. (b) Right – LANL MacroXRF instrument.

4. Results and Discussion

4.1 Handheld Zr Thickness Calibration

For each individual measurement the sum of the percentage composition of Zr, U, and Mo reported equaled $100.0\% \pm 0.01\%$, indicating that no spurious elements were tainting the calibration. Composition of the bare DU-10Mo plate, as reported by the handheld XRF, was 90.5 % U and 9.5 % Mo. Zr thickness as a function of detected elemental composition is shown in Figure 2. Empirical best-fit equations were generated for Zr thickness as a function of average

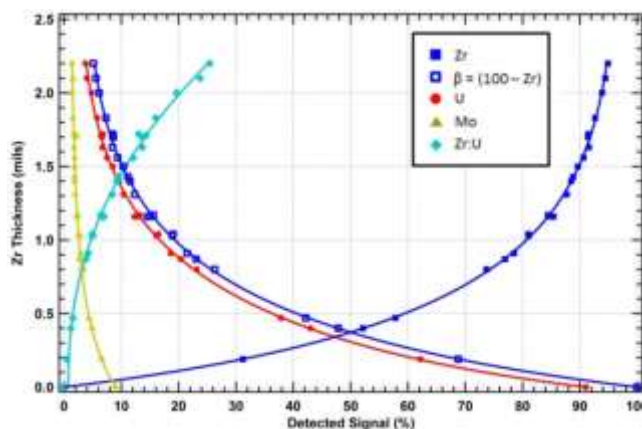


Figure 2: Zr thickness as a function of detected Zr, U and Mo signals, and as a function of the average ratio Zr:U.

detected U, Zr, Mo and Zr:U using built-in regression methods in IgorPro, a commercially-available scientific analysis software package that employs the Levenberg-Marquardt algorithm to fit data by searching for coefficients that minimize the value of χ^2 for a user-specified test function. A double-exponential function was found to be the best to fit to the U, Mo, and the

ratio Zr:U data, and to the Zr data when a reflection transformation $\beta = (100 - \text{Zr})$ was employed. Agreement between the Zr thickness measurement and the calculation based on individual and average U, Zr, or Zr:U data is $\pm 5\%$ or better (≤ 0.1 mil or 0.0025 mm). As long as the Zr thickness is ≤ 2.2 mils (0.056 mm), one can use the U, Zr or Zr:U data to extract the Zr coating thickness prior to the HIP process. Further details including calibration constants and extended error analysis are found in reference [14].

4.2 MacroXRF Zr Thickness Calibration

The measured intensity of the Zr- $K_{\alpha 1}$ line was plotted against known Zr foil thickness in mils. The resulting fit of the measured points was a logarithmic relationship with a correlation coefficient of 0.95. The log relationship indicates lower response of the Zr intensity with increasing thickness. The results for the target thickness of 1 mil (.025 mm) offers sufficient sensitivity to surpass the specified measurement of 1 mil \pm 0.5 mil (0.025 mm \pm 0.0125 mm).

4.3 Zr Thickness Measurements for RERTR Foil Samples

The handheld XRF was used to map Zr thickness across the front and back of a full-length (48") co-rolled foil. An 0.5" x 0.5" grid was placed on the surface of the foil and a 10-second XRF spectrum was taken at each intersection on the right and at 1" x 1" intervals on the left. After completion of the data gathering, elemental compositional results at each location were exported and the surface maps shown in Figure 3 were created using surface triangulation routines within the IDL Scientific Visualization Software package (Excelis VIS, Boulder CO). Results indicate fairly uniform Zr thickness averaging approximately 0.85 mils (0.022 mm), with a maximum variation of 0.2 mils (0.005 mm) over the back surface of the foil, less over the front surface. This is well within the targeted coating thickness specification.

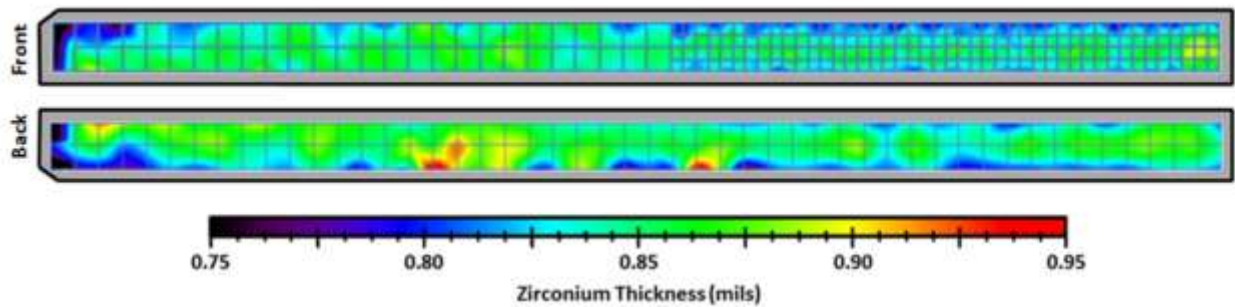


Figure 3: Zr thickness map for front (upper image) and back (lower image) surfaces of full-sized (48" x 3") Y12 RERTR foil 11K-635-A1. Individual 10-second XRF spectra were taken at the grid intersections indicated (1" x 1" on left side of front and entire back; 0.5" x 0.5" on right side of front). Zr thickness at each location was calculated from the elemental composition ratio Zr:U using a double exponential function, then interpolated to produce above map. Due to the large spot size of the handheld instrument and the uncoated foil edges, measurements start 0.5" in from the edges of foil.

In a similar manner, the handheld XRF method was used to assess the effect of cold-rolling on final Zr coating thickness. In the original experiment [4], five identical Zr/Du-10Mo/Zr sandwiches were subjected to different hot and cold rolling schedules as shown in Figure 4 to achieve a final foil thickness of 0.015" (0.38 mm). All foils were annealed at the same temperature and hold time. Ten-second XRF measurements were taken every 0.5" across the entire front and back surface of each foil as detailed above. Zr thickness was derived using the previously determined empirical thickness extraction algorithms based upon the ratio of measured Zr to U percentages and visual thickness maps were created using surface triangulation between each measurement point. Zr thickness measurement statistics are shown in Figure 5.

Note that because of the large spot size of the handheld instrument, there is a certain amount of intrinsic spatial averaging which tends to smooth out data values for high and low regions that are spatially compact.

For these samples, the average Zr thickness measured by handheld XRF ranged between 0.78 and 0.85 mils (0.020 – 0.022 mm), with greater cold work resulting in a slightly thicker Zr layer (increase of 9.4% with a 60% increase in cold work). The maximum Zr thickness variation across the surface of any given foil was 0.2 mil (0.005 mm), with the average Zr thickness being the same on both the front and back of each individual foil. Since the Zr coating on some of the foils showed obvious high and low spots, additional handheld measurements were taken at off-grid locations that exhibited significant surface roughness visually, although only marginal differences in readings were noted due to the small geometric area in question and the comparably large XRF spot size. Further details/images of the complete XRF analysis for the cold-rolling experiment are provided in reference [15].

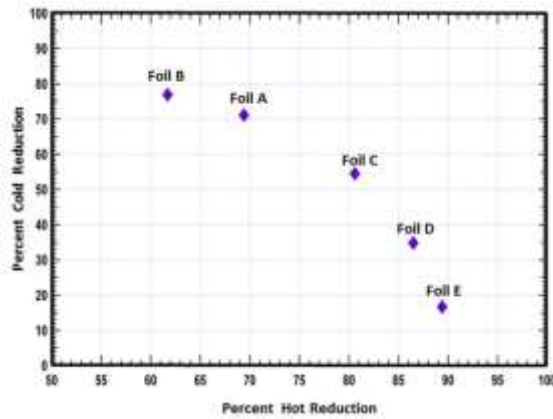


Figure 4: Rolling schedule for cold-rolling experiments. Each schedule selected to provide a final foil thickness of 15 mils.

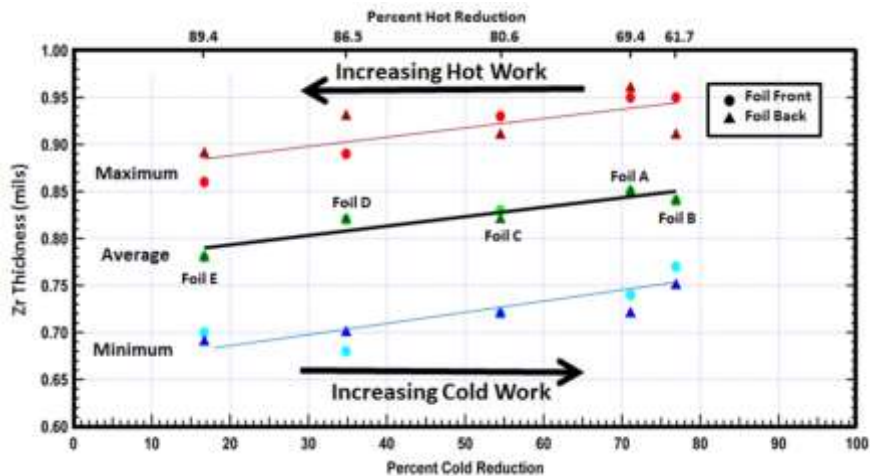


Figure 5: Minimum, maximum and average Zr coating thickness for cold-rolling study foils 13K-652 A - E, as measured by handheld XRF, as a function of percentage cold-work. All foils were subject to a variable but pre-determined amount of hot rolling (as indicated in rolling schedule) followed by cold rolling sufficient to ensure final foil thickness of 0.015"; Zr measurements were taken after completion of all hot and cold work.

For comparison, measurements for a single foil (Foil A) were also taken using the mXRF system with the 1 mm x 1mm spot size. In the latter case, sample density was increased from 0.5" to

0.25" horizontally. Thickness maps from the handheld and the mXRF measurements and corresponding measurement grids are shown in Figures 6 and 7. In Figure 6, each image is rendered using the identical color palette to enable direct comparison of absolute thickness, whereas in Figure 7 the palette is scaled to the minimum and maximum values of each dataset in order to emphasize location of the thicker and thinner regions in each measurement. To further facilitate numerical comparison, statistics for these samples are collated in Table 1.

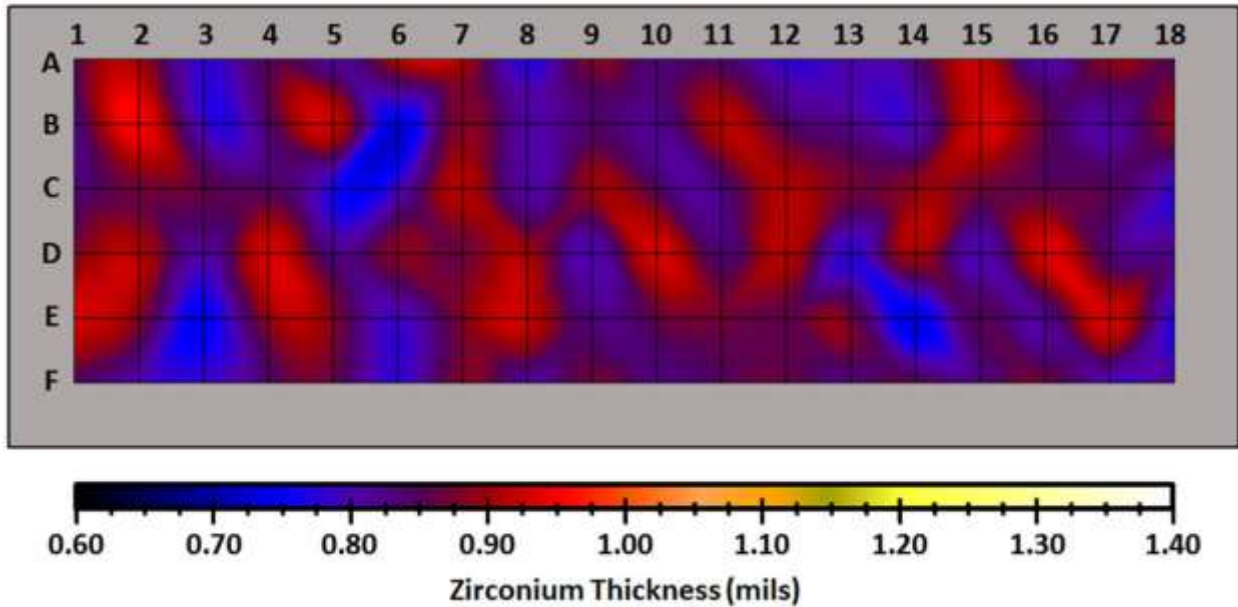


Figure 6(a): InnovX handheld XRF thickness map for the front side of Foil 13K-652-A. Sample density was 0.5" x 0.5", acquisition spot size was 5 mm x 7mm. Zr thickness was calculated from the ratio $R=Zr/U$ weight-percent composition.

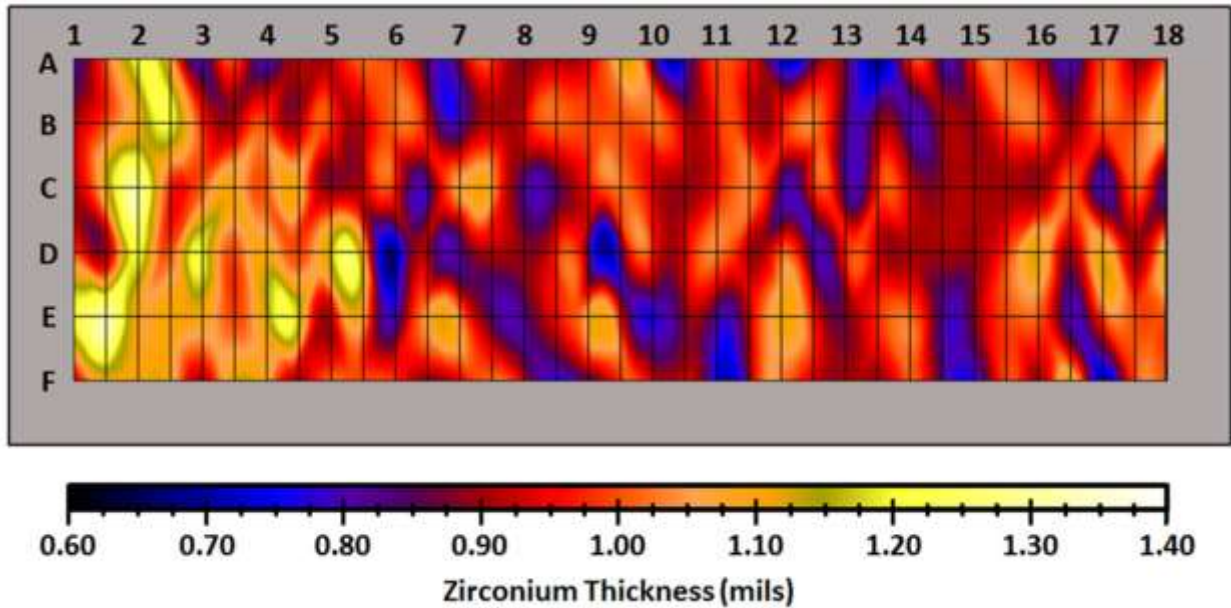


Figure 6 (b): MXRF thickness map for the front side of Foil 13K-652-A. Sample density was 0.25" x 0.5" using an acquisition spot size of 1 mm x 1mm. Zr thickness was calculated solely from the net intensity of the $Zr-K_{\alpha 1}$ line.

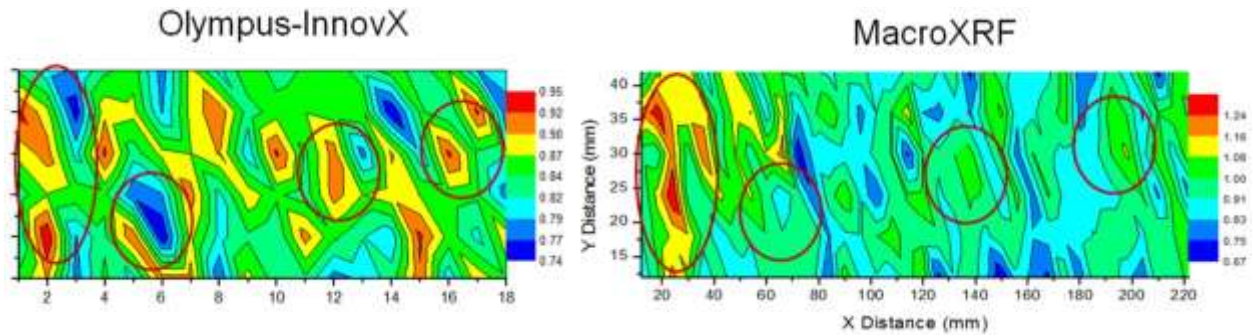


Figure 7: Zr thickness maps as in Figure 6, but with each image rendered such that the color palette is normalized to the minimum and maximum data values intrinsic to that specific dataset. In this representation, regardless of their absolute values, the thicker regions in each image appear in the yellow to red portions of the scale, mid-ranges are green and thinner regions appear blue. Note that in the image on the left, the palette range is 0.74 – 0.95 mils (~0.2 mils total), whereas on the right the range is 0.67-1.34 mils (~0.7 mils total). Red circles indicate qualitatively similar trends reported by both the handheld and the mXRF, although absolute measurements vary somewhat.

From looking at the visual images in Figures 6 and 7, it is apparent that both XRF instruments and calibration methods provide qualitatively similar data (*i.e.*, relatively thicker and thinner areas generally track each other) although there is a quantitative offset between the two. Obviously with its significantly smaller spot size the mXRF will be more sensitive to absolute differences in thickness over small areas, a fact that is reflected in the lower minimum and higher maximum values obtained using the mXRF instrument relative to those obtained using the handheld instrument and shown in Table 1. Note however that the average values differ by only 0.1 mil (0.0025 mm) or approximately 10% from each other. The agreement is quite good considering the measurements were done with two entirely different instruments using different calibration approaches. This illustrates the relative robustness of the XRF measurements.

Table 1: Comparison of MacroXRF and Olympus Handheld XRF Measurement of Cold-Rolling Study Sample 13K-652-A (Front)

	MXRF (240 points) mils	Handheld XRF (120 points) mils	Difference MXRF-Handheld mils [mm]
Min	0.7	0.74	-0.04 [-0.0010]
Max	1.33	0.95	0.38 [0.0097]
Avg.	0.95	0.85	0.10 [0.0025]
Range	0.63	0.21	0.42 [0.0107]
Std dev	0.11	0.05	0.06 [0.0015]

5. Conclusions

We have demonstrated that XRF is a viable means for providing accurate nondestructive measurements of Zr diffusion barrier layer thickness on RERTR fuel foils prior to HIP. Unlike current microscopy methods, which are time-consuming and can only examine cut foil edges, XRF methods are relatively quick and inexpensive and they provide quantitative information regarding Zr thickness distribution across the entire surface of the foil except perhaps at the very edges. Using foil standards of known thickness, XRF instruments may be calibrated to employ direct spectral intensity readings or elemental composition percentages, depending upon the output of the available instrument. With careful calibration and curve fitting, measurement

accuracy for both instruments is $\pm 5\%$ compared to standards. The average variation between the handheld and macroXRF measurements of the same sample, using two different calibration methods, was shown to be 0.1 mil (0.0025 mm) or approximately 10% of the known value when integrated over spatial dimensions greater than 1cm^2 . Although not explicitly covered in this paper, the XRF technique can also be calibrated to provide Al-6061 cladding thickness measurements for a known Zr coating, or simultaneous estimates of unknown Zr coating and Al cladding thickness; further details and comparison with ultrasonic assessment of Al cladding thickness are provided in reference [14].

Commercial handheld XRF analyzers are readily available, retailing for approximately \$50,000USD. Being small, quick, portable, and extremely accurate for compositional analysis, these instruments are ideal for thickness spot checks and *in situ* process monitoring on the shop floor. Because handheld XRF instruments are designed for contact or near contact measurements, the operator can be assured of relatively constant source-sample distance which in turn increases accuracy and repeatability and reduces the impact of sample waviness. On the other hand, handheld measurements are not easily amenable to automated scanning, and there does exist a potential for instrument contamination. The relatively coarse spot size ($\sim 1\text{cm}^2$) of standard commercial handheld XRF instruments results in measurements that are spatial averages about the measurement location, a feature that is generally desirable but which also means that small high and low spots or voids cannot be irrefutably detected or identified. The ability to characterize coatings at the edges of the fuel foil is similarly limited. Newer handheld instruments (*e.g.*, Bruker Tracer series) boast smaller spot sizes ($\sim 3\text{mm} \times 3\text{mm}$) and extremely high count rates which offer the possibility of higher sensitivity and greater speed; such instruments can also be custom-configured for quasi-automated data collection and scanning.

Scanning laboratory-grade XRF systems such as the LANL macroXRF instrument have the advantages of greater positional accuracy and generally more sensitive detectors, allowing for both repeatability and fully automated data collection, but there is a tradeoff in terms of cost, space and overall speed. The vastly smaller mXRF spot size ($\sim 1\text{mm}^2$ vs 1cm^2) can be advantageous in measuring closer to the foil edges, and also increases the ability of detecting small anomalous regions such as high and low spots or potential voids and/or porosity. Because the measurement is non-contact, it supports automated scanning, as noted above, and there are no concerns regarding potential contamination of the source/detector head. However, this also makes the resultant measurement extremely sensitive to sample flatness. Because the source/detector pair is suspended a fixed and considerable distance above the translational stage, the system has a relatively low count rate and is also sensitive to overall thickness of the sample.

Clearly both handheld XRF and laboratory-grade instruments such as the macroXRF have a place in the characterization of Zr diffusion barrier layers. When selecting an instrument for Zr thickness measurements, a scanning system such as the macroXRF is probably best used in R&D and large-scale production quality control and quality assurance applications due to the automated measurement capability, whereas a handheld XRF instrument is preferred for quick spot check applications at the point of manufacture.

6. Acknowledgements

The financial support of the US Department of Energy Global Threat Reduction Initiative Reactor Convert program is gratefully acknowledged. Los Alamos National Laboratory, an

affirmative action equal opportunity employer, is operated by Los Alamos National Security, LLC, for the National Nuclear Security Administration of the U.S. Department of Energy under contract DE-AC52-06NA25396. Foil samples and rolling data courtesy of Kester D. Clarke.

7. References

- [1] K.J. Hollis, "Zirconium Diffusion Barrier Coatings for Uranium Fuel used in Nuclear Reactors", *Advanced Materials & Processes*, Vol. 168, No. 11, Nov.–Dec. 2010, p 57-59.
- [2] K.J. Hollis, "Plasma Spraying of Diffusion Barrier Coatings for LEU Monolithic Fuel". RERTR 2012 – 34th International Meeting on Reduced Enrichment for Research and Test Reactors, Warsaw, Poland, October 14-17, 2012.
- [3] J.A. Smaga, J. Sedlet, C. Conner, M.W. Liberatore, D.E. Walker, D.G. Wygmans, G.F. Vandegrift, "Electroplating Fission Recoil Barriers onto LEU Metal Foils for Mo-99 Production Targets," *Proceedings of the 20th International Meeting on Reduced Enrichment for Research and Test Reactors*, Jackson Hole, WY, October 5-10, 1997.
- [4] D.J. Alexander, K.D. Clarke, J.E. Scott, J.D. Montalvo, D.E. Dombrowski, "Effect of Cold Deformation and Annealing Temperature on U-10Mo Fuel Foil Geometry", RRFM 2014 European Research Reactor Conference, Ljubljana, Slovenia, March 30 – April 3, 2014. LA-UR-14-21384.
- [5] Richard M. Rousseau, Fundamental algorithm between concentration and intensity in XRF analysis. *X-RAY SPECTROMETRY 13(3) 115-120* (1984).
- [6] Y. Kataoka, Standardless X-Ray Fluorescence Spectrometry (Fundamental Parameter Method using Sensitivity Library). *The Rigaku Journal 6(1):33-40* (1989).
- [7] D. K. G. De Boer, et al. How accurate is the Fundamental Parameter approach? XRF analysis of bulk and multi-layer samples. *X-Ray Spectrometry, 23: 33-28* (1993).
- [8] H. A. Van Sprang, Fundamental Parameter Methods in XRF Spectroscopy. *Advances in X-ray Analysis, Vol.42*, JCPDS-International Centre for Diffraction Data (2000).
- [9] A.G. Karydas, et al. Modeling XRF intensities for portable/handheld analyzers using Fundamental Parameters approach. Paper F-37, *Denver X-Ray Conference*, 6-10 August 2012, Denver CO (2012).
- [10] G. Cliff, and G.W. Lorimer, The quantitative analysis of thin specimens. *Journal of Microscopy, 103: 203–207* (1975).
- [11] C. Fiorini, et al. Determination of the thickness of coatings by means of a new XRF spectrometer. *X-Ray Spectrum, 31:92-99* (2002).
- [12] EDAX Corporation, Coating thickness and composition analysis by micro-EDXRF. Application Note: XRF, available online at <http://www.edax.com/download/Orbis%20Coating%20Thickness%20and%20Composition%20by%20Micro%20XRF-1.pdf>, accessed 22 March 2012.
- [13] Heather M. Volz, George J. Havrilla, Robert M. Aikin, Jr., Velma M. Montoya, "Macroscopic X-ray Fluorescence Capability for Large Scale Elemental Mapping," *Advances in X-ray Analysis, 54*, 2011, *Proceedings of the 59th Annual Conference on Applications of X-ray Analysis*, August 2-6, 2010, Denver, CO, 280-288.
- [14] D.A. Summa, "Handheld XRF for Mapping Zr Coating and Al-6061 Cladding Thickness in RERTR Fuel Elements", Los Alamos National Laboratory Unclassified Technical Report, Dec. 7, 2012. LA-UR-12-28620.
- [15] D.A. Summa, K.D. Clarke, "Cold Rolling Study: Zr Thickness via Handheld XRF", FFC Quarterly Technical Review, Lynchburg VA, Jan. 14-15, 2014. LA-UR-14-20164.